

## THERMOGRAPHY: PRINCIPLES AND APPLICATIONS

MERCEDES SOLLA<sup>1</sup> & SUSANA LAGÜELA<sup>2</sup>

<sup>1</sup> DEFENSE UNIVERSITY CENTER, SPANISH NAVAL ACADEMY, MARÍN, SPAIN  
MERCHISOLLA@CUD.UVIGO.ES

<sup>2</sup> UNIVERSITY OF SALAMANCA, DEPARTMENT OF CARTOGRAPHIC AND TERRAIN ENGINEERING,  
ÁVILA, SPAIN  
SULAGUELA@USAL.ES

### ABSTRACT

*This tutorial presents the main principles of the thermography technique and the civil-engineering applications of this non-destructive testing method. Several examples are given and two case studies are presented, where thermography and Ground Penetrating Radar are jointly used to assess a radiant heating floor installed in a building, and to detect moisture in a masonry arch bridge.*

**KEYWORDS:** Thermography; Ground Penetrating Radar; Non-destructive testing; Civil engineering.

### 1. FUNDAMENTALS OF THERMOGRAPHY

Infrared thermography is a non-destructive testing method based on the capacity of measuring temperature values from the radiation emitted by bodies in the thermal-infrared range of the electromagnetic spectrum.

The infrared range consists of four different bands, as shown in Table 1. The 5 – 7  $\mu\text{m}$  band is not included in the table because it corresponds to the so-called ‘low transmittance window,’ where infrared radiation is not transmitted through the atmosphere. The 7 – 14  $\mu\text{m}$  band, denominated ‘Thermal Infrared’ (TIR) can be related to temperature values. In particular, bodies that emit radiation in the TIR band have a temperature over absolute zero (0 K; -273.15 °C).

**TABLE 1 – INFRARED BAND OF THE SPECTRUM**

| Band                           | Wavelength ( $\mu\text{m}$ ) |
|--------------------------------|------------------------------|
| Near Infrared (NIR)            | 0.4 – 1                      |
| Short-wave Infrared (SWIR)     | 1 – 3                        |
| Mid-wavelength infrared (MWIR) | 3 – 5                        |
| Thermal Infrared (TIR)         | 7 – 14                       |

A thermographic camera captures radiation in the thermal infrared band and gives information about the temperature of the body under study. The radiation is received as an electric signal by the sensor, and its magnitude is directly related to the temperature of the body. The relationship between radiation and temperature is defined by the Stefan-Boltzmann law:

$$W_{bb} = \sigma T^4 \quad (1)$$

where  $W_{bb}$  is the radiation emitted by a black body,  $\sigma$  is Stefan-Boltzmann constant, equal to  $5.67 \cdot 10^{-8}$  W/m<sup>2</sup>K, and  $T$  is the temperature of the black body. This law is implemented in the camera, so that the user receives directly a temperature value per pixel.

Every object receives radiation from the Sun and surrounding elements, which acts in different ways once it reaches the object. The radiation arriving to an object is therefore divided into:

- ❑ Absorbed radiation. This is the portion of radiation that enters the object and changes its thermal condition, and consequently its temperature.
- ❑ Reflected radiation. This is the portion of radiation that does not enter the object.
- ❑ Transmitted radiation. This is the portion of radiation that enters the objects and travels through it without causing any important effect in the object.

The radiation outgoing from an object consists of emitted, reflected and transmitted radiations. The reflected radiation goes towards sources in front of the object, while the transmitted radiation goes to bodies behind the object. The emitted radiation can be associated to absorbed radiation: the absorbed radiation changes the thermal state of the body, and then the body emits radiation proportional to its temperature. This fraction of radiation is commonly denoted by the term 'emissivity' and represented by the symbol  $\varepsilon$ . Transmitted radiation is considered as null for non-transparent bodies: for such bodies, outgoing radiation consists of the emitted and reflected portions, only.

The emissivity is an essential parameter to be taken into account for a correct calculation of a real-body temperature with respect to the temperature of a black body. A black body is an unreal object with a

perfect behaviour regarding emittance; thus, all radiation emitted by a black body is the result of its temperature, without a reflected portion. For this reason, the emissivity value of a black body is 1, while real bodies present emissivity values from 0.1 to 0.99. Because total radiation is quantified as 1, the portion of radiation that is not emitted, is reflected. Thus, bodies with high reflectivity present low emissivity, and vice versa. For example, construction materials commonly present emissivity between 0.9-0.96; non-oxidized metals present low emissivity, ranging between 0.2 and 0.5 [1]. Regarding temperature calculation, emissivity is introduced in Stefan-Boltzmann law as follows:

$$W_{bb} = \varepsilon\sigma T^4 \quad (2)$$

The emissivity value of materials can be extracted from tables [1], through the simultaneous measurement of the object under study and a piece of black tape with known emissivity [2], or by direct computation based on Equations (1) and (2), by using apparent temperature values measured with a camera and real temperature values measured with a contact thermometer [3].

In addition to emissivity, other factors influence the quantity of radiation emitted by each body (see Figure 1), as well as the quantity of radiation received by the camera. The attenuation effect of the atmosphere on the infrared radiation coefficient is taken into account to correct the computation of the temperature value. This attenuation coefficient depends on three factors: distance to the objects from the camera, ambient temperature and relative humidity.

Deeper explanation about fundamentals and principles of infrared thermography are found in the literature [3, 4].

## 2. CLASSIFICATION OF THERMOGRAPHIC APPROACHES

There are two classifications of infrared thermography methods, based on the possible presence of a heat source, on the relative positions between camera, object under study and heat source, and on the importance given to the temperature value (e.g., whether temperature differences or temperature absolute values are measured and interpreted). More details are given in the following sub-sections.

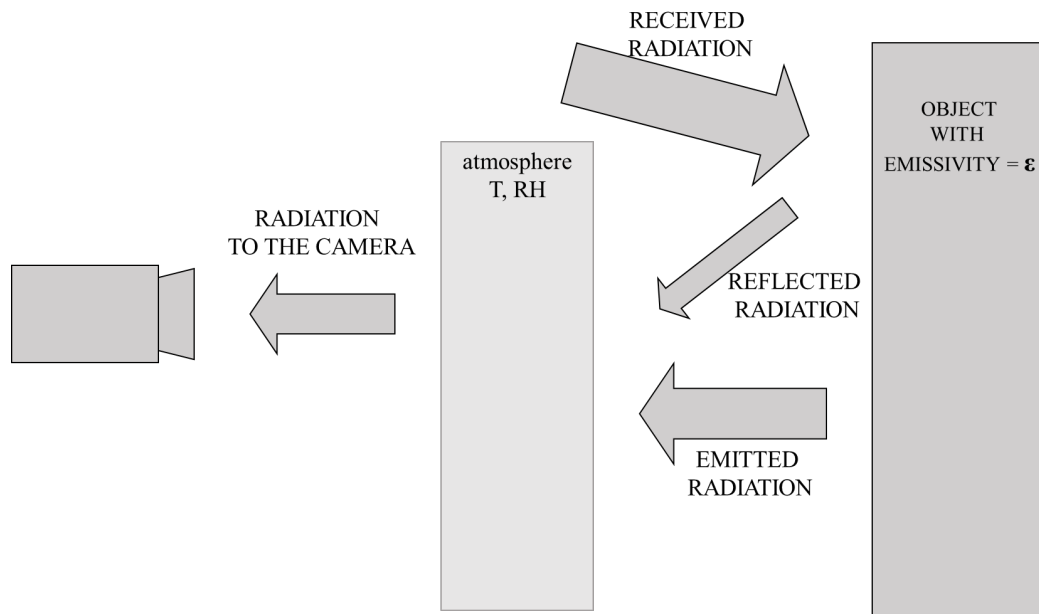


**FIG. 1** – Distribution of infrared radiation [3].

## 2.1. ACTIVE VERSUS PASSIVE APPROACHES

- ❑ Passive thermography: no external heat source is used. The camera measures the radiation of the objects under test in their normal state, that is, under the usual conditions of received radiation. The Sun is not considered as an external heating source in this classification, due to its natural presence, but of course its presence (or absence) is important for the correct development of the study.
- ❑ Active thermography: implies the use of an artificial heat source. The heat source can vary from pulsed laser and flash lamps [5, 6], to non-optical sources such as mechanical vibration, acoustic wave excitation and microwaves [7-9]. Active thermography is divided into transmission-mode thermography and reflection-mode thermography, depending on the relative positions between camera, object and heat source, and the consequent origin of the radiation measured (see Figure 2).

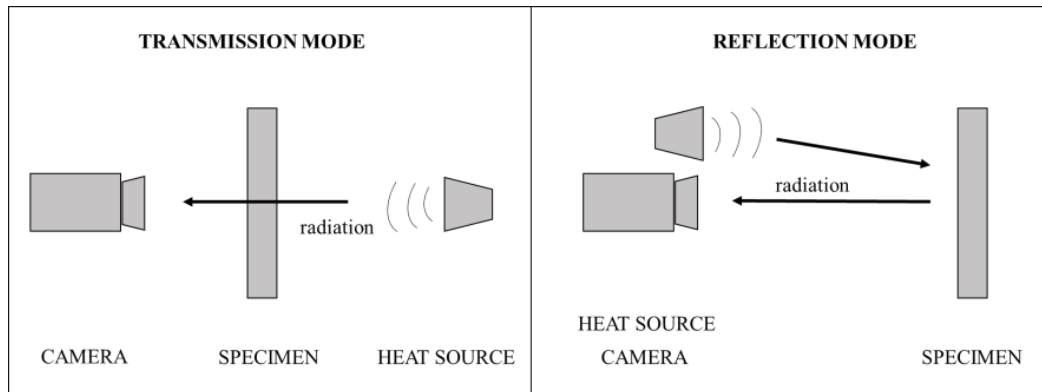


**FIG. 2** – Configuration of transmission and reflection mode thermography, for active thermography [3].

## 2.2. QUALITATIVE VS QUANTITATIVE APPROACHES

- ❑ Qualitative thermography is focused on the search of thermal pathologies in the objects, based on temperature differences instead of temperature values. Thus, in this approach, the evaluation of real absolute temperatures is not the objective of the study and relative temperatures are measured. In this way, the presence of thermal anomalies can be detected.

*E.g.: detection of moisture areas in buildings.*

- ❑ Quantitative thermography is an approach based on the accurate measurement of temperature values. This method requires the application of both emissivity and ambient compensations, as well as a careful data acquisition, taking into account every factor of influence such as the presence of reflectors and air currents. This approach allows the evaluation of the severity of the problems and the thermal characterization of the objects.

*E.g.: identification of pathology as a critical or a medium problem, estimation of thermal diffusivity of a material.*

Qualitative studies are based on passive thermography; whereas quantitative analysis is based on both passive and active approaches.

### **3. CIVIL ENGINEERING APPLICATIONS OF INFRARED THERMOGRAPHY**

#### **3.1. BUILDING INSPECTION**

Possible tasks performed in buildings, where infrared thermography finds application, are:

- Detection of structural defects, such as joint failure, cracking, delamination/detachment and moisture/efflorescence [10-12].
- Detection of thermal bridges, i.e., areas where heat transfer is facilitated due to the construction weakness (e.g. no insulation in junctions between walls and the building envelop) [13].
- Detection of tightness weaknesses, allowing the escape of heated air from the interior (e.g. no sealing around elements such as windows, free space under doors) [14].
- Detection of air infiltration, similar to the previous failure but allowing the entrance of exterior air in the building (e.g. around windows and doors without sealing)[14].
- Detection of building installations and pathologies (e.g. electricity, plumbing) [15].

As an example, Figure 3 presents two thermal images showing: a case of lack of insulation around the windows, and of thermal bridge between the facade and roof, where red/yellow colours indicate higher temperatures or heated air from the interior (left panel); a case of air infiltration where dark blue colours indicate lower temperatures or colder air entering from the exterior (right panel).

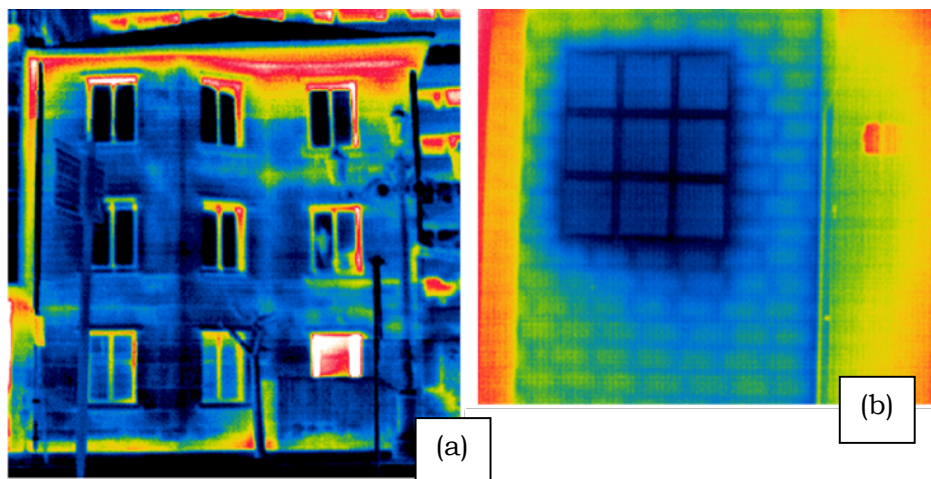
#### **3.2. CIVIL INFRASTRUCTURE INSPECTION**

Possible tasks performed in civil infrastructure assessment, where infrared thermography finds application, are:

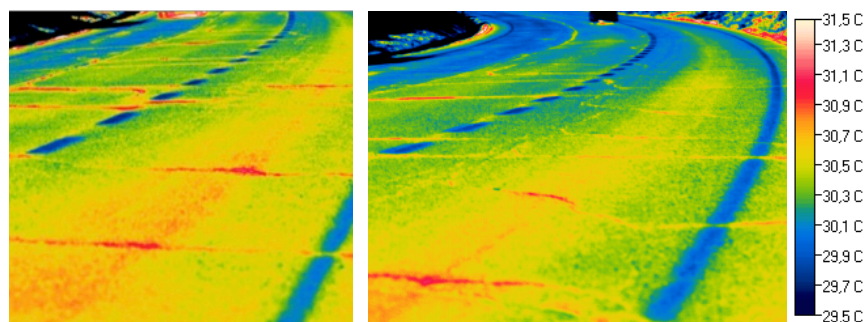
- Security and safety issues, such as pedestrian [16] or vehicle [17] recognition, which was the first application of infrared thermography as a night-vision tool.
- Inspection of pavement (e.g. cracks) [18].
- Diagnosis of bridges and tunnels (e.g. moisture or delamination areas in concrete bridges) [19-22].

Figure 4 illustrates an example of cracking in asphalt pavement. The presence of cracks is associated with red colour, given that cracks allow the accumulation of air inside, and the inspection was performed during a day with ambient temperature around 31°C.

Figure 5 shows an example of a masonry arch bridge inspected by means of infrared thermography. In the thermal images, colours go from dark red for the lowest temperatures, to red, light red, orange, yellow and white for the highest temperatures. The analysis of the thermal images leads to the detection of moisture in the central part of the arch, and near the border with the pathway. The presence of water becomes more evident in the downstream wall of the same arch (left), where water can be detected all around the arch in spite of the presence of a large quantity of vegetation hiding part of the faults.



**FIG. 3** –Examples of (a) lack of insulation around windows and (b) air infiltration from the exterior of the building.



**FIG. 4** –Example of cracking in asphalt pavement.

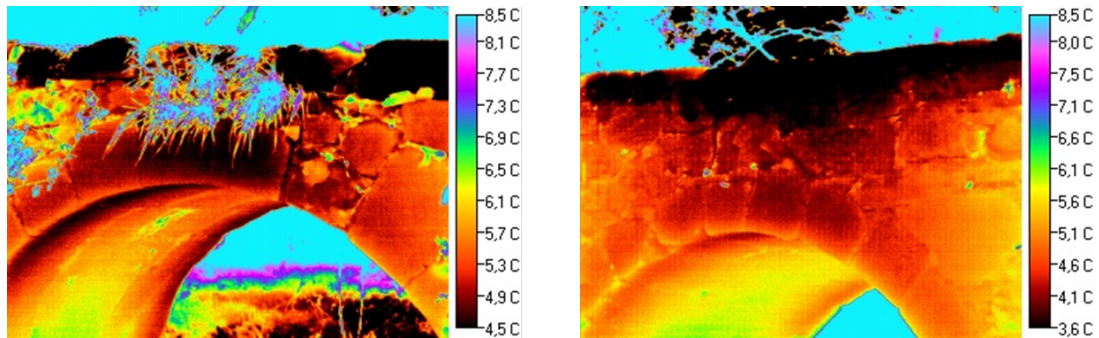


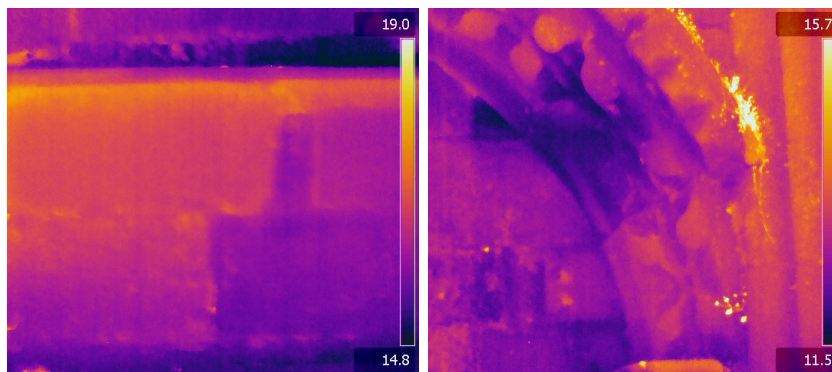
**FIG. 5** –Example of thermographic survey to detect moisture in a masonry bridge: downstream wall on the left, upstream wall on the right.

### 3.3 INSPECTION OF HERITAGE SITES

Possible tasks where infrared thermography finds application are:

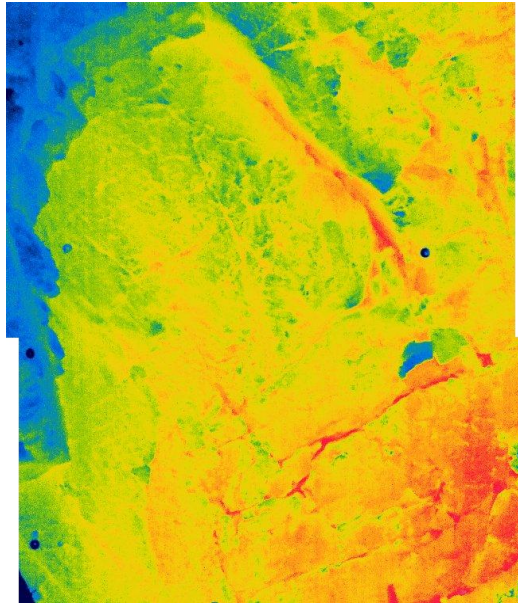
- Identification of archaeological remains due to the presence of subsurface air cavities [23, 24].
- Diagnosis of paintings and murals (e.g. cracks, holes, voids) [25, 26].
- Monument conservation (moisture, cracks, temperature evolution) [27-29].

Figure 6 shows thermal images acquired in the ruins of a historic church. Most pathologies detected in the inspection were structural (loose rocks, left panel) and presence of moisture with different levels of severity (right panel).



**FIG. 6** – Example of thermographic survey in the ruins of a historic church. Thermal images show a loosened stone (left), presence of moisture within the masonry, efflorescence and moss (right).

Figure 7 is a thermal image of a cave painting in Cáceres (Spain). The objective of the study is to determine the ambient conditions of the cave in order to evaluate the need of measures to optimize the conservation of the paintings. Blue colour is associated to the lowest temperatures, with increasing temperatures corresponding to green, yellow and red.



**FIG. 7** – Thermal image of a cave painting, showing an increasing trend for the temperature from top to bottom of the cave.

#### **4. COMBINING INFRARED THERMOGRAPHY AND GROUND PENETRATING RADAR**

##### **4.1. DETECTION OF BUILDING INSTALLATIONS (RADIANT HEATING FLOOR) [30]**

###### **Infrared thermography**

- The thermographic survey was developed with an active approach, in the transmission mode, as the installation is used as heating source.
- The installation was turned on 5 h before the inspection, with the aim to reach a 5-10°C temperature difference between the pipelines and the surrounding environment. The existence of a temperature difference allows for the determination of thermal anomalies due to defects in the installation.

- The thermographic inspection was performed by using a NEC TH9260 camera with a 640\*480UFPA sensor, having a 0.06°C resolution and  $\pm 2^\circ\text{C}$  accuracy.
- A single image could not cover the dimensions of the grid or area under study. Three different thermal images were therefore acquired to create a thermographic mosaic covering the whole area.
- In order to avoid reflections, their main source, lamps, were off during the inspection. In addition, the camera operator was located at a  $90^\circ$  angle so that the reflection by his body did not affect the measurement.

The results of the investigation are shown in Figure 8.

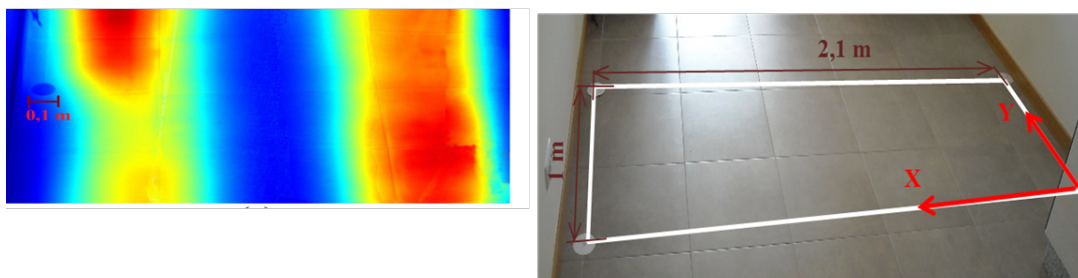


**FIG. 8** – Thermographic mosaic (adapted from [30]) on the left; dark red colours represent higher temperatures (pipeline paths). Photo of the inspect surface on the right.

### Ground Penetrating Radar

- A ProEx Ground Penetrating Radar (GPR) system was used, with a 2.3-GHz antenna. This frequency was selected because, in the considered scenario, it provides a signal penetration depth of about 40 cm and a vertical resolution of about 1-2 cm.
- The survey was carried out with a 2-cm spatial sampling and a 12-ns time window.
- An encoder-based wheel was attached to the antenna, as a distance measurement instrument, to measure the profile length and to control the 2 cm spatial sampling.

- The data were collected with the antenna polarization orthogonal to the longitudinal direction of the heating pipelines (X direction in the right panel of Figure 8).
- Three-dimensional (3D) data acquisition of equidistant parallel profiles, at regular intervals of 5 cm, was done.

The results of the investigation are shown in Figure 9.

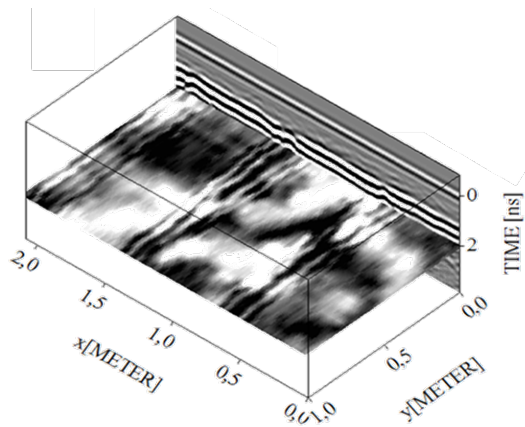


**FIG. 9** – Results of the GPR survey (adapted from [30]).

### **Discussion of the results and integrated interpretation**

- GPR provided information about the number of pipelines and distribution. In particular, GPR data revealed the presence of three pipelines.
- The thermographic mosaic showed the presence of two pipelines.
- The spatial correspondence between radargram and thermographic mosaic (see Figure 10) leads to the conclusion that the central pipeline is not working.
- GPR gives information about all pipelines but cannot distinguish whether they are working or not. Thermography can detect only the working installations.
- The different thermal print between the pipelines on the left and on the right shows a malfunctioning of the pipeline on the left, given its colder temperature distribution.

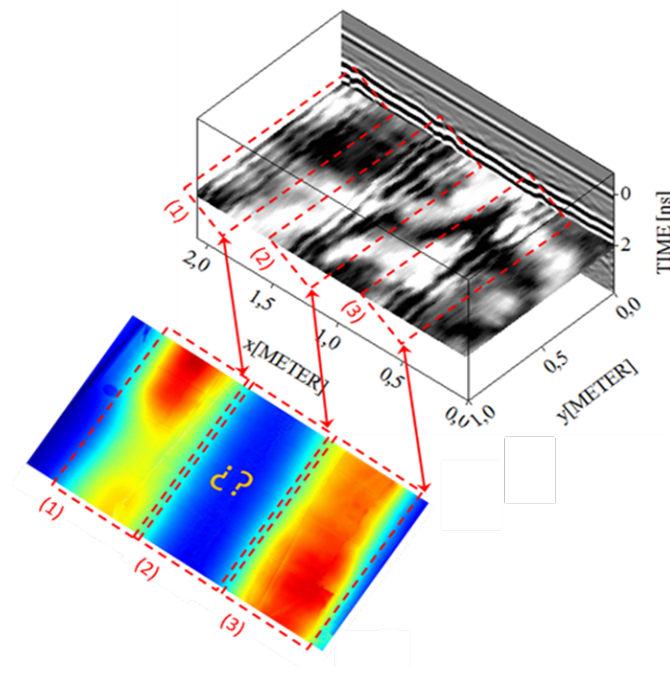


**FIG. 10** – Comparison of 3D GPR data and thermographic mosaic (adapted from [30]).

## 4.2. DETECTION OF MOISTURE IN MASONRY ARCH BRIDGES [31]

### Infrared thermography

- The thermographic survey was developed with a passive approach.
- The passive solar radiation was used to increase the evaporation rate of water inside the structure and to maximize the temperature difference between moist and dry areas thanks to the evaporation process.
- Environment conditions were: a temperature of 10°C, with 40% relative humidity.
- Object distance: ~ 5m (see Figure 11(a)).
- Emissivity value: 0.80 (test in situ).
- The thermographic inspection was performed by using a NEC TH9260 camera with a 640\*480UFPA sensor, with 0.06°C resolution and ±2°C accuracy.

- The thermographic survey included the walls of the bridge (both upstream and downstream walls) and the inner part of the vault of the arch under study.
- The temperature interval selected was from 6 to 12°C, with colours going from dark red for the lowest temperatures, to red, light red, orange, yellow and white for the highest temperature (see Figure 11(b)).
- The thermal images obtained were also registered in a 3D model (see Figure 11(d)), enabling the study of the complete vault instead of studying each thermal image separately, thus reducing the confusion caused by the lack of reference points in individual images.
- The 3D model was provided through photogrammetric approaches, by using a digital camera Nikon D200 (see Figure 11(c)).
- Finally, in order to avoid the effects of the perspective view, each wall, upstream and downstream, were orthogonally projected to the parallel plane, and the corresponding orthothermograms were obtained (see Figure 11(e)).

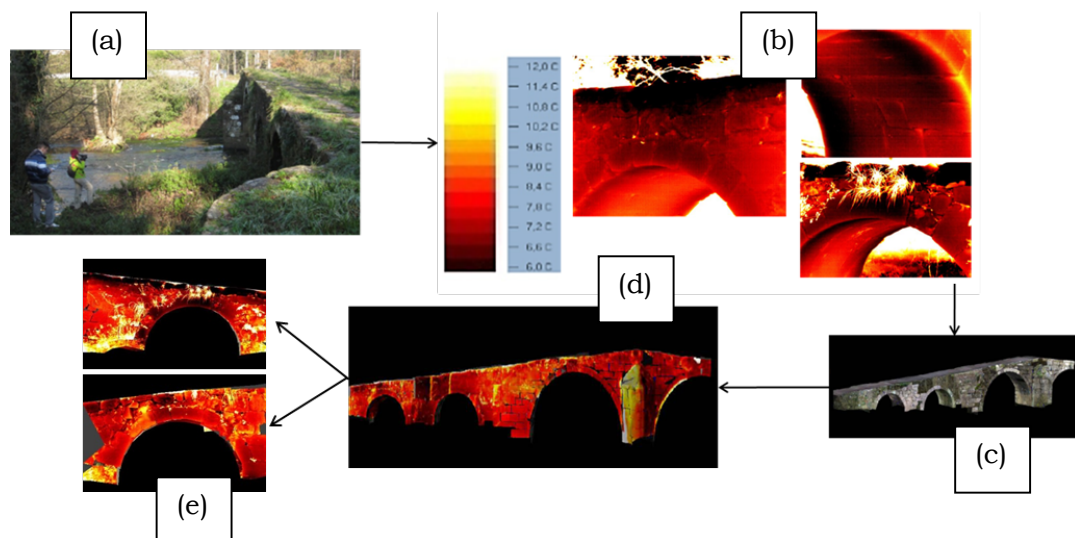


**FIG. 11** – Results of the thermographic survey: (a) data acquisition, (b) orthothermograms, (c) 3D model with RGB texture, (d) 3D model with thermographic texture, and (e) orthothermograms of the arch under study.

## Ground Penetrating Radar

- The GPR data were collected with a RAMAC/GPR CU-II system.
- The 1-GHz antenna was chosen because it provides a signal penetration depth of about 1 m and a vertical resolution of about 4 cm.
- The survey parameters were: 2-cm spatial sampling and 45-ns time window.
- The GPR survey was carried out passing the GPR antenna around the internal surface of the vault (see Figure 12) in order to avoid scattering and complex reflection patterns produced by the heterogeneous filling commonly used during construction.
- An encoder-based wheel was attached to the back of the antenna to measure the profile lengths as well as to control the spatial sampling.



**FIG. 12** – 1-GHz GPR data acquisition through the intrados of the vault arch.

### Results and combined interpretation:

- The orthothermograms of both the upstream and downstream walls of the bridge were obtained from the thermographic 3D model.
- The thermography results facilitated the identification of probable moist areas in the bridge surface as those having lower temperatures (dark red). This is due to the cooling effect of evaporation on the surface where it takes place.

- Important evidence of moisture appears on the upper part of the walls, near the border with the road, and in the masonry over the arch (Figure 13(a)).
- GPR provided information on the inner materials of the bridge. Observing the radargram, a stronger reflection generated from the backfill/stone interface can be noted (red arrow in Fig. 13(b)), which is clearly visible only in the zones contiguous to the keystone of the arch ( $\approx$  at 20 ns). The most probable explanation is that water could be accumulated there.
- The GPR interpretation agreed with the thermographic data obtained, which showed a more critical presence of water (dark red areas) around the keystone, more pronounced towards the face of the upstream wall.

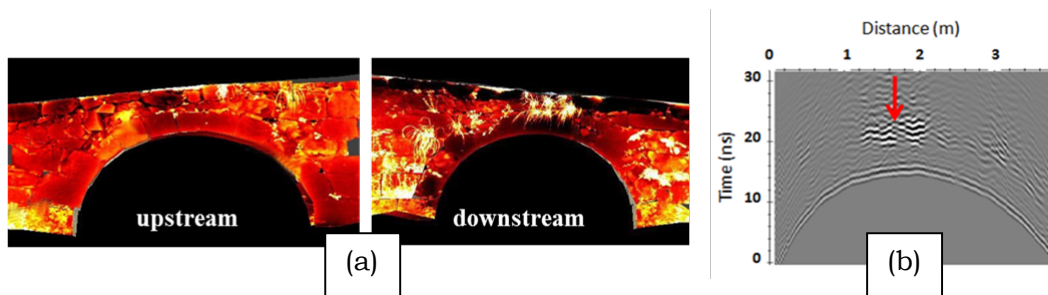


**FIG. 13** – (a) Orthothermograms obtained from both the upstream and downstream walls of the bridge and (b) 1-GHz GPR data.

## 5. CONCLUSIONS

Thermal infrared thermography has proved to be an adequate technique for detecting and analysing faults and pathologies that can affect heat transfer. Although the technique only provides information from the surface of the objects, different procedures allow the extraction of information from the subsurface, such as heating from an external source (Sun radiation or artificial sources).

Thermal infrared thermography is a good complementary technique to Ground Penetrating Radar (GPR), both prior and during the GPR inspection. In the first case, infrared thermography can provide information about the presence of water or the conductivity of the material under study, so that the GPR processing can be optimized. In

the second case, infrared thermography can yield information concerning the most superficial part of the inspected object, where the GPR signal can be less accurate than in deeper regions. Thus, both techniques can be used jointly to perform a more exhaustive analysis about the state of constructions.

## ACKNOWLEDGEMENTS

The results presented in this work were possible thanks to the support provided by the Applied Geotechnologies Research Group from the University of Vigo (Spain). The authors would also like to thank the Ministry of Economy and Industry of the Government of Spain, for their support given via the human resources grant FPGI-2013-17516. This tutorial is a contribution to the EU funded COST Action TU1208.

## REFERENCES

- [1] T. Suesut, N. Nunak, T. Nunak, A. Rotruga, and Y. Tuppadung, "Emissivity measurements on material and equipment in electrical distribution system," International Conference on Control, Automation and Systems, Gyeonggi-do, South Korea, October 2011.
- [2] P. Fokaides, S. Kalogirou, "Application of infrared thermography for the determination of the overall heat transfer coefficient (U-value) in building envelopes", Applied Energy, vol. 88, pp. 4358-4365, 2011.
- [3] S. Lagüela, L. Díaz-Vilariño, and D. Roca, "Infrared thermography: fundamentals and applications," book chapter in Non-destructive techniques for the evaluation of Structures and Infrastructures (Eds. B. Riveiro and M. Solla), CRC/Balkema, Taylor & Francis Group, 2016.
- [4] C. Meola and G. Carlomagno, "Recent advances in the use of infrared thermography", Measurement Science and Technology, vol. 15, pp. 27-58, 2004.
- [5] L. Teng, D. Almond, D. Andrew and S. Rees, "Crack imaging by scanning pulsed laser spot thermography", NDT&E International, vol. 44, pp. 216-25, 2011.
- [6] N. Tsopeles, N. Siakavellas, "Experimental evaluation of electromagnetic-thermal non-destructive inspection by eddy current thermography in square aluminium plates", NDT&E International, vol. 44, pp. 609-620, 2011.

- [7] L. Favro, X. Han, Z. Ouyang, G. Sun, H. Sui, R. Thomas, "Infrared imaging of defects heated by a Sonic pulse", *Review of Scientific Instruments*, vol. 71, pp. 2418-2421, 2000.
- [8] F. Mabrouki, M. Thomas, M. Genest, A. Fahr, "Numerical modelling of vibrothermography based on plastic deformation", *NDT&E International*, vol. 43, pp. 476-483, 2010.
- [9] S. Keo, F. Brachelet, F. Breaban and D. Defer, "Steel detection in reinforced concrete wall by microwave infrared thermography", *NDT&E International*, vol. 62, pp. 172-177, 2014.
- [10] Ch. Maierhofer, R. Arndt, M. Röllig, C. Rieck, A. Walther, H. Scheel, and B. Hillemeier, "Application of impulse-thermography for non-destructive assessment of concrete structures," *Cement and Concrete Composites*, vol. 28(4), pp. 393-401, 2006. ]
- [11] S. Bagavathiappan, B.B. Lahiri, T. Saravanan, J. Philip, and T. Jayakumar, "Infrared thermography for condition monitoring – A review," *Infrared Physics & Technology*, vol. 60, pp. 35-55, 2013.
- [12] M.R. Clark, D.M. McCann, and M.C. Forde, "Application of infrared thermography to the non-destructive testing of concrete and masonry bridges," *NDT & E International*, vol. 36(4), pp. 265-275, 2003.
- [13] F. Bianchi, A. Pisello, G. Baldinelli, and F. Asdrubali, "Infrared thermography assessment of thermal bridges in building envelope: experimental validation in a test room setup," *Sustainability*, vol. 6(10), pp. 7107-7120, 2014.
- [14] C.A. Balaras, and A.A. Argiriou, "Infrared thermography for building diagnostics," *Energy and Buildings*, vol. 34, pp. 171-183, 2012.
- [15] N. Laaidi, S. Belattar, and A. Elbaloutti, "Pipeline corrosion, modelling and analysis," *Journal of Nondestructive Evaluation*, vol. 30(3), pp. 158-163, 2011.
- [16] M. Khozium, A. Abuarafah, and E. AbdRabou, "A proposed computer-based system architecture for crowd management of pilgrims using thermography," *Life Science Journal*, vol. 9(2), pp. 277-282, 2012.
- [17] Y. Iwasaki, S. Kawata, and T. Nakamiya, "Robust vehicle detection even in poor visibility conditions using infrared thermal images and its application to road traffic flow monitoring," *Measurement Science and Technology*, vol. 22(8), 085501 (10pp), 2011.
- [18] M. Solla, S. Lagüela, and H. González-Jorge, "Approach to identify cracking in asphalt pavement using GPR and infrared thermographic

methods: Preliminary findings,” *NDT&E International*, vol. 62, pp. 55-65, 2014.

[19] J. Dumoulin, A. Crinière, and R. Averty, “The detection and thermal characterization of the inner structure of the Musmeci bridge deck by infrared thermography monitoring,” *Journal of Geophysics and Engineering*, vol. 10(6), 064003 (11pp), 2013.

[20] M. Matsumoto, K. Mitani, F. Catbas, and S. Hayashi, “On-site application of innovative bridge inspection methods using image processing and infrared technology,” 7th International Conference on Bridge Maintenance, Safety and Management, Shanghai, China, July 2014.

[21] T. Sakagami, “Remote non-destructive evaluation technique using infrared thermography for fatigue cracks in steel bridges,” *Fatigue and Fracture of Engineering Materials and Structures*, vol. 38(7), pp. 755-779, 2015.

[22] G. Barla, F. Antolini, and G. Gigli, “3D Laser scanner and thermography for tunnel discontinuity mapping,” *Geomechanics and tunnelling*, vol. 9(1), pp. 29-36, 2016.

[23] B. Lunden, “Aerial thermography: a remote sensing technique applied to detection of buried archaeological remains at a site in Dalecarlia, Sweden,” *Geografiska Annaler*, vol 67(1), pp. 161-166, 1985.

[24] J. Casana, J. Kantner, A. Wiewel, and J. Cothren, “Archaeological aerial thermography: a case study at the Chaco-era Blue J community, New Mexico,” *Journal of Archaeological Science*, vol. 45, pp. 207-219, 2014.

[25] F. Mercuri, U. Zammit, N. Orazi, S. Paoloni, M. Marinelli, and F. Scudieri, “Active infrared thermography applied to the investigation of art and historic artefacts,” *Journal of Thermal Analysis and Calorimetry*, vol. 104, pp. 475-485, 2011.

[26] E. Kordatos, D. Exarchos, C. Stavrakos, A. Moropoulou, and T. Matikas, “Infrared thermographic inspection of murals and characterization of degradation in historic monuments,” *Construction and Building Materials*, vol. 48, pp. 1261-1265, 2013.

[27] E. Rosina, and J. Spodek, “Using infrared thermography to detect moisture in historic masonry: a case study in Indiana,” *APT Bulletin*, vol. 34(1), pp. 11-16, 2003.

[28] A. Kandemir-Yucel, A. Tavukcuoglu, and E. Caner-Saltik, “In situ assessment of structural timber elements of a historic building by infrared thermography and ultrasonic velocity,” *Infrared Physics & Technology*, vol. 49, pp. 243-248, 2007.

- [29] E. Rosina, S. Della Torre, P. Gasparoli, L. Lazzaroni, L. Di Bella, A. Castiglioni, M. Radaelli, and C. Sotgia, "Localizing historical clues using IRT and petrographic analysis at Villa Mirabello, Monza (Italy)," *Archaeometry*, vol. 51(5), pp. 715-732, 2009.
- [30] S. Lagüela-López, M. Solla-Carracelas, L. Díaz-Vilariño, and J. Armesto-González, "Inspection of radiant heating floor applying non-destructive testing techniques: GPR and IRT," *DYNA Colombia*, 82(190), pp. 221-226, 2015.
- [31] M. Solla, S. Lagüela, B. Riveiro, and H. Lorenzo, "Non-destructive testing for the analysis of moisture in the masonry arch bridge of Lubiáns (Spain)," *Structural Control and Health Monitoring*, vol. 20, pp. 1366-1376, 2013.